

## Article

# Eddavidite, $\text{Cu}_{12}\text{Pb}_2\text{O}_{15}\text{Br}_2$ , a New Mineral Species, and Its Solid Solution with Murdochite, $\text{Cu}_{12}\text{Pb}_2\text{O}_{15}\text{Cl}_2$

Melli Rosenblatt <sup>1,\*</sup>, Marcus J. Origlieri <sup>2</sup>, Richard Graeme III <sup>3,†</sup>, Richard Graeme IV <sup>3</sup>, Douglas Graeme <sup>3</sup> and Robert T. Downs <sup>1</sup> 

<sup>1</sup> Department of Geosciences, University of Arizona, Tucson, AZ 85721, USA; rdowns@arizona.edu

<sup>2</sup> Mineral Zone, 1370 N. Silverbell Rd. #140, Tucson, AZ 85745, USA; marcus@mineralzone.com

<sup>3</sup> Graeme Reference Library, P.O. Box 4272, Bisbee, AZ 85603, USA

\* Correspondence: rose.melli@gmail.com

† Deceased.

**Abstract:** Eddavidite is a new mineral species (IMA2018-010) with ideal formula,  $\text{Cu}_{12}\text{Pb}_2\text{O}_{15}\text{Br}_2$ , and cubic  $\text{Fm}\bar{3}\text{m}$  symmetry:  $a = 9.2407(9) \text{ \AA}$ ;  $V = 789.1(2) \text{ \AA}^3$ ;  $Z = 2$ . Eddavidite is the bromine analog of murdochite,  $\text{Cu}_{12}\text{Pb}_2\text{O}_{15}\text{Cl}_2$ , with which it forms a solid solution series. The type locality is the Southwest mine, Bisbee, Cochise County, Arizona, U.S.A. Eddavidite also occurs in the Ojuela mine, Mapimí, Durango, Mexico. Eddavidite occurs as domains within mixed murdochite–edavidite crystals. The empirical formula, normalized to 12 Cu apfu, is  $\text{Cu}_{12}(\text{Pb}_{1.92}\text{Fe}_{0.06}\text{Si}_{0.06})(\text{O}_{15.08}\text{F}_{0.02})\text{-(Br}_{0.99}\text{Cl}_{0.89}\square_{0.12})$ . Type locality samples contain up to 67% eddavidite component, while Ojuela mine samples contain up to 62%. Mixed eddavidite–murdochite crystals show forms {100} and {111}; the habit grades from cubic through cuboctahedral to octahedral. Mixed eddavidite–murdochite crystals exhibit good cleavage on {111}. Eddavidite is black, opaque with submetallic luster, and visually indistinguishable from intergrown murdochite. Its Mohs hardness is 4;  $d_{\text{meas.}} = 6.33 \text{ g/cm}^3$ ,  $d_{\text{calc.}} = 6.45 \text{ g/cm}^3$ . The crystal structure, refined to  $R = 0.0112$ , consists of corner-sharing square planar  $\text{CuO}_4$  units, arranged in  $\text{Cu}_{12}\text{O}_{24}$  metal oxide clusters, which encapsulate Br atoms.  $\text{PbO}_8$  cubes share edges with  $\text{Cu}_{12}\text{O}_{24}$  clusters in a continuous framework. Eddavidite incorporates bromine remaining after desiccation of paleo-seawater at its two known localities, which were both once situated along the Western Interior Seaway.



**Citation:** Rosenblatt, M.; Origlieri, M.J.; Graeme, R., III; Graeme, R., IV; Graeme, D.; Downs, R.T. Eddavidite,  $\text{Cu}_{12}\text{Pb}_2\text{O}_{15}\text{Br}_2$ , a New Mineral Species, and Its Solid Solution with Murdochite,  $\text{Cu}_{12}\text{Pb}_2\text{O}_{15}\text{Cl}_2$ . *Minerals* **2024**, *14*, 307. <https://doi.org/10.3390/min14030307>

Academic Editors: Irina O. Galuskina, Igor V. Pekov and Zhenyu Chen

Received: 1 December 2023

Revised: 31 January 2024

Accepted: 31 January 2024

Published: 15 March 2024



**Copyright:** © 2024 by the authors. Licensee MDPI, Basel, Switzerland. This article is an open access article distributed under the terms and conditions of the Creative Commons Attribution (CC BY) license (<https://creativecommons.org/licenses/by/4.0/>).

**Keywords:** eddavidite; murdochite; new mineral; crystal structure; lead copper oxide; Br; bromine; Ojuela mine; Mexico; Bisbee; Arizona; paleo-seawater; Western Interior Seaway

## 1. Introduction

The recognition of eddavidite arises from decades of investigations into the ontology of murdochite. Murdochite was first described from the Mammoth mine, Tiger, Arizona in 1955 [1,2]. Wet chemical analysis found major lead, copper, and oxygen. A contemporaneous crystal structure model was based upon that of rock salt, with a unit cell content of 32 O atoms in cubic closest packed arrangement and 32 concomitant octahedral sites occupied by an ordered arrangement of 24 Cu, 4 Pb, and 4 vacancies. However, the crystal structure solution gave a poor reliability factor ( $R \sim 0.17$ ) [3]. The original description and separate crystal structure study both gave a stoichiometric formula for murdochite:  $\text{Cu}_6\text{PbO}_8$  [2,3]

Two independent investigations, both published in 1970, evinced certain complexities in the mineral murdochite. One study [4] showed pronounced zoning under reflected light in material from Anarak, Iran. Microprobe analysis revealed higher Pb in bright zones than in dark zones, with  $\text{PbO}_2$  and CuO content variations of 2.2 wt.% and 0.9 wt.%, respectively. It was concluded that Cu contents varied inversely with Pb contents, albeit non-stoichiometrically [4]. The other study [5] revealed significant Cl and Br for the first time in murdochite, in samples from both the Hansonburg district, New Mexico, and Anarak, Iran [5]. Pronounced zoning under reflected light was again noted; however, this

was attributed to variable Cl/Br ratios [5]. Assuming that halogens substitute for oxygen, a non-stoichiometric formula for murdochite was proposed with excess cations and fixed total anions:  $\text{Cu}_{6\pm x}\text{Pb}_{1\pm x}(\text{O},\text{Cl},\text{Br})_8$  [5].

A redetermination of the murdochite crystal structure in 1983 found Cu in typical 4 + 2 coordination, consisting of 4 equatorial Cu-O bonds of 1.921 Å and 2 apical halogen separations at 3.261 Å. Pb is coordinated by eight O atoms at the corners of a cube, with Pb-O separations of 2.283 Å [6]. The refinement assumed full occupancy of a halogen site, which is distinct from an O site constrained to 0.94 (=15/16) occupancy for charge balance [6]. The model converged well ( $R = 0.027$ ). A non-stoichiometric formula with anion vacancies was proposed for murdochite:  $\text{Cu}^{2+}_6\text{Pb}^{4+}_8\text{O}_{8-x}(\text{Cl},\text{Br})_{2x}$  ( $x \leq 0.5$ ) [6].

The deprecated murdochite structural model from 1955 [3] lives on in solid-state chemistry and condensed matter physics literature, i.e., “murdochite-type”  $\text{Ni}_6\text{MnO}_8$  [7]. The accepted structure for the mineral specs murdochite [6] and also for eddavidite appears in synthetic cuprates:  $\text{Cu}_6\text{O}_8\text{InCl}$ ,  $\text{Cu}_6\text{O}_8\text{In}(\text{Cl},\text{NO}_3)$ , and  $\text{Cu}_6\text{O}_8\text{YCl}$  [8,9], as well as in the palladate  $\text{Tl}^{3+}\text{Pd}^{2+}_6\text{O}_8\text{Tl}^{1+}$  [10]. DFT modeling [11] indicates that murdochite would favor a structure with Jahn–Teller distortion typical of  $\text{Cu}^{2+}$  [6]. Nevertheless, the term “murdochite structure” in scientific literature refers variously to the rock salt model with Pb and Cu in regular octahedral coordination [3] or the model with 4 + 2 coordinated Cu and 8 coordinated Pb atoms [6].

While analyzing a museum sample of Bisbee murdochite (Figure 1), backscattered electron (BSE) imaging showed pronounced zoning. Standardized WDS analysis found domains with atomic Br > Cl. Single-crystal X-ray diffraction study indicated a unit cell similar to that of murdochite, though somewhat larger. The new mineral and its name received approval from the Commission on New Minerals, Nomenclature and Classification (CNMNC) of the International Mineralogical Association (IMA2018-010).

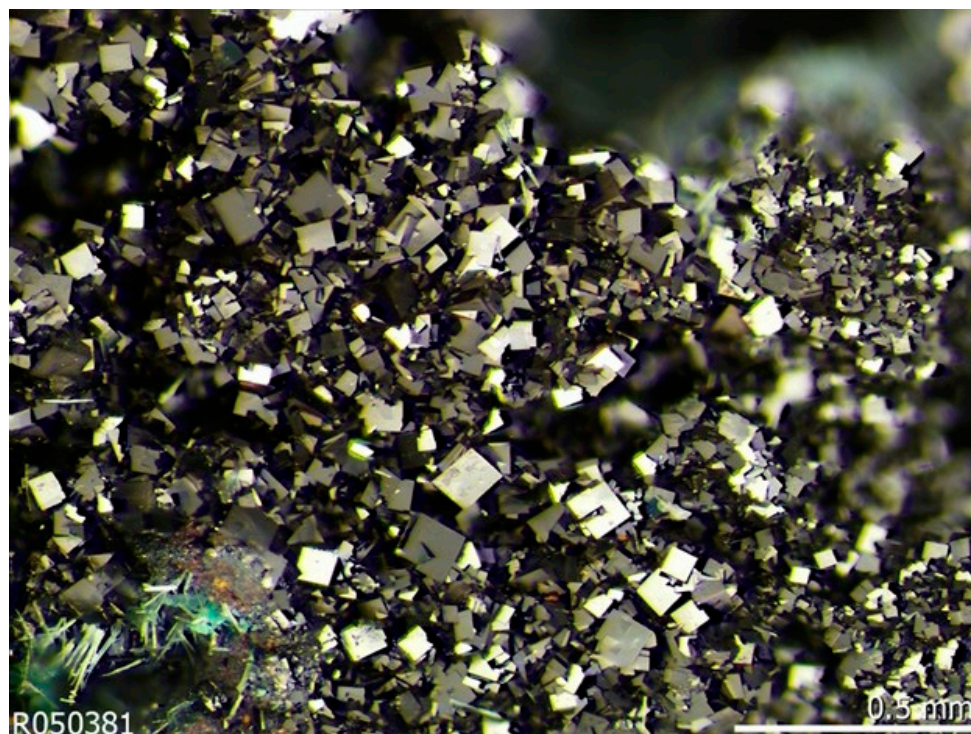


**Figure 1.** Type eddavidite forms domains in mixed murdochite–eddavidite crystals, seen here with minor acicular malachite. Locality: Southwest mine, Bisbee, Cochise County, Arizona. Sample: University of Arizona Gem & Mineral Museum 12326 (holotype).

This study both characterizes the new mineral species eddavidite and further delineates its solid solution series with murdochite. The holotype sample is on deposit at the

University of Arizona Alfie Norville Gem & Mineral Museum with catalog number 12326 (Figure 1); co-type fragments thereof are on deposit with the RRUFF Project as sample R050381 (Figure 2).

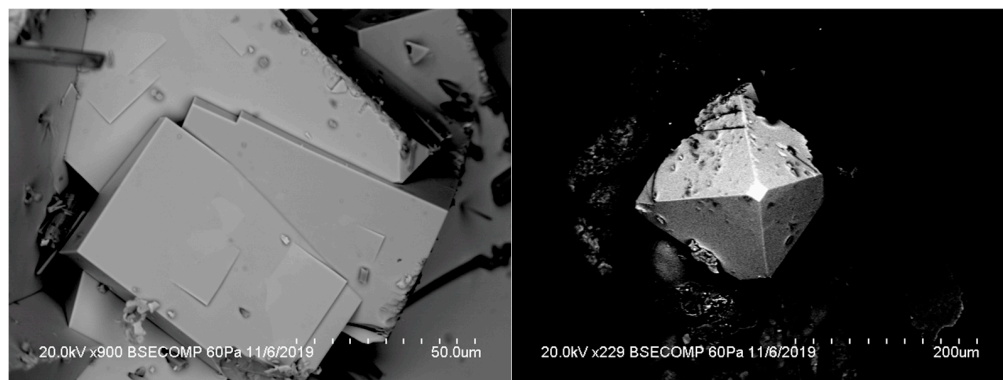


**Figure 2.** SEM imagery of mixed eddavidite–murchisonite crystals. **(left)** Simple cubic crystals. This sample has a maximum molar Br/(Br + Cl) = 0.64 (Table S1). Locality: Southwest mine, Bisbee, Cochise County, Arizona, U.S.A. Sample: RRUFF R050381 (co-type). **(right)** Octahedral crystal with minor cubic modifications. This sample has a maximum molar Br/(Br + Cl) = 0.52 (Table S1). Locality: Ojuela mine, Mapimí, Durango, Mexico. Sample: NHMLAC 38450.

The mineral name eddavidite honors Dr. Edward Emil “Ed” David (1925–2017). Dr. David sought to make science more relevant and accessible to the public; he received much recognition in the scientific, technical, and professional communities. Dr. David worked at Bell Labs from 1950 to 1970, eventually rising to Executive Director of Communications Systems Research. U.S. President Nixon tapped Dr. David to serve as National Science Advisor from 1970 to 1973. He also sat on NASA’s Advisory Council and served as the U.S. Representative to the NATO Science Committee [12]. In 1973, Dr. David went to work in the private sector, later becoming President of Exxon Research Corporation in 1977, from which he retired in 1986.

Dr. David became interested in mineral collecting at the age of six when his uncle “Bibby” presented him with a wooden box of mineral specimens. That gift ignited a lifelong passion in Dr. David, who later built a fine mineral collection, the “core” of which went to the Houston Museum of Natural Science in 1995 [13]. Unflinchingly, Dr. David started assembling another mineral collection. Dr. David donated 36 fine copper specimens in 2014 and arranged a posthumous gift of his remaining ~450 specimens to the University of Arizona Mineral Museum, the predecessor of the University of Arizona Alfie Norville Gem & Mineral Museum (ANGMM). Dr. David served on the University of Arizona Mineral Museum advisory board from 2007 to 2017, and the ANGMM currently features a gallery of his former specimens.

## 2. Materials and Methods

Electron probe microanalyses were performed in WDS mode on a Cameca SX-100 electron microprobe, housed at the Department of Lunar and Planetary Sciences, University of Arizona, with an accelerating voltage of 15 kV, an operating current of 20 nA, and a ~10 µm beam diameter. Standards used were Cu (cuprite from Bisbee, inhouse standard); Pb (NBS glass K0229); Cl (Brazilian scapolite, USNM R6600-1 containing 1.43% Cl); Br (synthetic CsBr); F (synthetic MgF<sub>2</sub>); Si (San Carlos Fo<sub>92</sub> olivine, inhouse standard); Fe (fayalite from Rockport, MA); Cd (Cd metal); K (orthoclase supplied by Penn State); and Ca (anorthite from Hakone, Japan). Data reduction followed the PAP method [14]. The normalization of eddavidite formulae differs from that for rock-forming minerals [15], which is based on total anions. For this reason, eddavidite and murchisonite formulae were calculated on the basis of 12 Cu apfu (Tables 1 and S1). Additional BSE imaging employed a

Hitachi 3400N SEM at Arizona LaserChron Center, Department of Geosciences, University of Arizona.

**Table 1.** Chemistry of co-type eddavidite-murdochite used for crystal structure refinement. The empirical formula is  $\text{Cu}_{12}(\text{Pb}_{1.92}\text{Fe}_{0.06}\text{Si}_{0.06})(\text{O}_{15.08}\text{F}_{0.02})(\text{Br}_{0.99}\text{Cl}_{0.89}\square_{0.12})$ , when normalized to 12 Cu. Locality: Southwest mine, Bisbee, Cochise County, Arizona, U.S.A. Sample R050381.

	Spot Range (wt. %)	Mean of 9 (with s.d.)
PbO <sub>2</sub>	25.35–31.31	29.74(189)
CuO	58.07–65.61	61.71(194)
SiO <sub>2</sub>	0.17–0.37	0.23(8)
FeO	0.09–0.59	0.30(16)
F	0.00–0.06	0.02(2)
Cl	1.52–3.91	2.04(74)
Br	2.80–6.19	5.11(108)
total		<b>99.15</b>
<b>molar Br/(Br + Cl)</b>	<b>0.64–0.24</b>	<b>0.53</b>
# spots eddavidite	-	<b>6</b>
# spots murdochite	-	<b>3</b>

An X-ray diffraction study was conducted with a Bruker APEX II diffractometer at the Department of Geosciences, University of Arizona. The X-ray generator produces MoK $\alpha$  radiation at 45 kV and 40 mA, which is monochromated by a graphite crystal, concentrated by Monocap capillary X-ray optics, and collimated to a width of 350  $\mu\text{m}$ . The unit cell parameters refined from the powder data are  $a = 9.2424(67)$  Å,  $V = 789.5(17)$  Å<sup>3</sup>, calculated using in-house software [16]. The X-ray powder diffraction profile appears in Table 2.

**Table 2.** X-ray diffraction data ( $d$  in Å) for type eddavidite, compared with those of murdochite [3]. The X-ray diffraction profiles of eddavidite and murdochite are nearly indistinguishable.

$d_{\text{obs}}$ (Eddavidite)	$I_{\text{obs}}$	$d_{\text{calc}}$ (Eddavidite)	$d_{\text{obs}}$ (Murdochite)	{hkl}
5.296	40	5.336	5.30	{111}
4.739	15	4.621	4.59	{200}
3.260	9	3.268	3.25	{220}
2.788	5	2.787	2.776	{311}
2.668	100	2.668	2.659	{222}
2.305	31	2.311	2.303	{400}
2.120	13	2.120	2.109	{331}
2.063	6	2.067	2.059	{420}
1.882	3	1.887	1.880	{422}
1.773	2	1.779	1.772	{333}, {511}
1.632	35	1.634	1.629	{440}
1.561	6	1.562	1.556	{531}
1.536	3	1.540	1.537	{442}, {600}
1.456	2	1.461	1.457	{620}
1.394	28	1.393	1.404	{622}
1.334	7	1.334		{444}
1.292	3	1.282		{640}
1.154	5	1.155		{800}
1.060	11	1.060		{662}

A quarter sphere of single-crystal X-ray diffraction intensity data were collected from a  $70 \times 60 \times 60$   $\mu\text{m}$  crystal fragment. The structure was solved with direct methods, using SHELX-2017 [17]. The chemistry of the crystal used in the refinement is given in Table 2. All reflections were indexed with a cubic unit cell. The crystal structure refinement was fixed to the empirical halogen composition:  $\text{Cu}_{24}\text{Pb}_4\text{O}_{30.20}\text{Br}_{1.98}\text{Cl}_{1.78}$ . Details of the crystal structure refinement are given in Table 3; atomic coordinates and displacement parameters appear in Tables 4 and 5.

**Table 3.** Crystal structure refinement details for eddavidite (this study) and murdochite [6].

	Eddavidite	Murdochite
locality	Southwest mine, Bisbee, Arizona	Hansonburg district, New Mexico
crystal size	70 × 60 × 60 μm	90 × 110 × 90 μm
idealized formula	Cu <sub>12</sub> Pb <sub>2</sub> O <sub>15</sub> Br <sub>2</sub>	Cu <sub>6</sub> PbO <sub>8-x</sub> (Cl,Br) <sub>2x</sub>
refined unit cell content	Cu <sub>24</sub> Pb <sub>4</sub> O <sub>30.20</sub> Br <sub>1.98</sub> Cl <sub>1.78</sub>	Cu <sub>24</sub> Pb <sub>4</sub> O <sub>30</sub> (Cl <sub>0.64</sub> Br <sub>0.36</sub> ) <sub>4</sub>
space group	Fm $\bar{3}$ m	Fm $\bar{3}$ m
a (Å)	9.2407(9)	9.224(2)
V (Å <sup>3</sup> )	789.1(2)	784.3(3)
R	0.0112	0.027
wR	0.0348 *	0.026
maximum 2θ (°)	66.6	100
{hkl} span	−13 < h < 4 −5 < k < 13 −14 < l < 1	--
# reflections collected	490	1723
# independent reflections	105	258
# reflections I > 2s(I)	105	255
# parameters refined	9	10
R <sub>int</sub>	0.0151	--
GoF	1.316	--
r(Pb-O) (Å)	2.286(3)	2.283(1)
r(Cu-O) (Å)	1.9245(7)	1.921(1)
r(Cu-X) (Å)	3.2671(3)	3.261(2)
X site chemistry	0.495 Br + 0.445 Cl	0.64(2) Cl + 0.36 Br

\*  $w = 1/[\sigma^2(F_{\text{obs}}^2) + (0.0148P)^2 + 5.7163P]$  where  $P = (F_{\text{obs}}^2 + 2F_{\text{calc}}^2)/3$ ; \* X site chemistry fixed to empirical results for eddavidite; refined for murdochite.

**Table 4.** Atomic positions and site occupancies (fixed for refinement) for eddavidite.

Site	Occupancy	Wyckoff	x	y	z
Cu	Cu <sub>1.00</sub>	24(d)	¼	¼	0
Pb	Pb <sub>1.00</sub>	4(a)	0	0	0
O	O <sub>0.944</sub>	32(f)	0.1428(2)	x	x
X	Br <sub>0.495</sub> Cl <sub>0.445</sub>	4(b)	½	½	½

**Table 5.** Isotropic equivalent and anisotropic displacement parameters for eddavidite.

Atom	U <sub>eq.</sub>	U <sub>11</sub> = U <sub>22</sub>	U <sub>33</sub>	U <sub>12</sub>	U <sub>13</sub> = U <sub>23</sub>
Cu	0.00524(18)	0.0056(2)	0.0046(3)	−0.00222(18)	0
Pb	0.00420(14)	0.00420(14)	U <sub>11</sub>	0	0
O	0.0025(5)	0.0025(5)	U <sub>11</sub>	0.0006(6)	U <sub>12</sub>
X	0.0237(5)	0.0237(5)	U <sub>11</sub>	0	0

### 3. Results

#### 3.1. Description

All eddavidite recognized to date occurs as domains in mixed eddavidite–murdochite crystals. Mixed eddavidite–murdochite crystals show cubic {100} and octahedral {111} forms (Figures 1–3) and combinations thereof (Figures 2 and 3). The maximal crystal sizes observed to date are ~100 μm at Bisbee and ~300 μm at Ojuela. Eddavidite is black, opaque, and submetallic. The streak is black. Eddavidite is visually indistinguishable from coexisting murdochite. Its Mohs hardness is 4. Eddavidite–murdochite is brittle, showing good cleavage on {111}. The measured density is 6.33 g/cm<sup>3</sup>. The density calculated from the crystal structure refinement is 6.45 g/cm<sup>3</sup>. At present, only chemical analyses can reliably distinguish eddavidite from murdochite.



**Figure 3.** Mixed murdochite-eddavidite crystals up to 300  $\mu\text{m}$  with aurichalcite, showing a combination of cubic {100} and octahedral {111} forms. This sample has maximal molar  $\text{Br}/(\text{Br} + \text{Cl}) = 0.62$  (Table S1). Locality: Ojuela mine, Mapimí, Durango, Mexico. Sample: RRUFF R110122.

### 3.2. Occurrence and Paragenesis of Eddavidite–Murdochite

The occurrence of eddavidite is correlated with that of murdochite; eddavidite is only known as domains within mixed eddavidite–murdochite crystals. Murdochite occurs in several mines of the Bisbee mining area, Cochise County, Arizona. Murdochite was first recorded in the Higgins mine in 1955 [3], which was the only Bisbee occurrence reported as late as 1981 [18]. In 1993, three additional occurrences of murdochite were reported from Bisbee: one in the Shattuck mine and two in the Southwest mine [19]. The Graeme family collection also includes murdochite samples from the Uncle Sam, Copper Queen, Holbrook and Cole mines. Murdochite from the Cole mine is associated with rosasite and malachite (Graeme sample R3494). A sample from the Shattuck mine has proven to be murdochite intergrown with plattnerite (Graeme sample 1483). Apart from the Cole mine, the aforementioned mines are tightly grouped in the northwestern portion of the Bisbee mining area [19]. In fact, the Copper Queen, Higgins, Holbrook, Shattuck, Southwest, and Uncle Sam mines comprise a single network of interconnected subterranean workings.

The type locality of eddavidite is the 5th level of the Southwest mine in the Bisbee mining area. Cavities containing eddavidite–murdochite occur in *limonite* pods hosted by Mississippian Escabrosa limestone, formed by fugitive fluids associated with Jurassic porphyry copper mineralization [20]. *Limonite* is a field term for intermixed iron oxides-hydroxides not discriminated by laboratory analysis; hematite and goethite are major components. The type occurrence of eddavidite is a large open pocket,  $\sim 150' \times \sim 25'$ , located at the intersection of the Czar fault and an unnamed fault. Towards the 54th crosscut on the 5th level of the Southwest mine, there is minor malachite, and the stope ceiling is covered in later plumose, cream-colored calcite. While most of the *limonite* is pulverent massive, rare *limonite* casts of former gypsum crystals are also present. Mixed murdochite–eddavidite crystals form both directly on *limonite* and are also perched on acicular malachite, all of which precede a late generation of bladed calcite. The holotype sample follows the sequence *limonite*  $\rightarrow$  malachite  $\rightarrow$  murdochite–eddavidite  $\rightarrow$  calcite. Nearby in this same orebody, cuprite nodules host fine cuprite crystals and a suite of exotic copper species, including atacamite, claringbullite, nantokite, paratacamite, and spangolite [19]. Surprisingly, unit cell determination and SEM-EDS chemistry of supposed claringbullite from the Southwest mine revealed its identity as barlowite (RRUFF sample R110007).

During this investigation, microprobe analysis found eddavidite domains in murdochite dominated crystals from the Ojuela mine complex, Mapimí mining district, Durango, Mexico. The Ojuela mine exploits oxidized Pb-Ag ores consisting of cerussite and argentiferous galena [21,22]. Attractive specimens of wulfenite and mimetite are recovered as a byproduct of artisanal lead-silver mining [23]. The first record of murdochite in the Ojuela mine is a mere listing in a 1956 paper describing an unrelated zinc arsenate [24]. Murdochite occurs in a complex assemblage with aurichalcite, calcite, hydrozincite, hemimorphite, malachite, plattnerite, and rosasite. While not specifically associated with eddavidite, and not found all together on a single specimen, each of these species occurs in contact with murdochite. Also known in this assemblage are scrutinyite [25], fluorite, and baryte; none of which have yet been observed in association with murdochite (or eddavidite). Two samples containing eddavidite from the Ojuela mine are recognized in this study: RRUFF R110122 (Figure 3), which is associated with aurichalcite, and NHMLAC 38450 (Table S1).

### 3.3. Eddavidite–Murdochite Chemistry

The chemical data (Tables 1 and S1) indicate an essentially binary solid solution from 96% murdochite component to 69% eddavidite component. Figure 4 shows the remarkable variation in both Pb/Cu (ideally 2/12 apfu Cu) and molar Br/(Br + Cl) for murdochite–eddavidite. The spots with molar Br/(Br + Cl) > 0.5 are eddavidite, while those < 0.5 are murdochite. Curiously, analyses of eddavidite–murdochite are characteristically non-stoichiometric (Tables 1 and S1). Crystal structure analysis indicates the presence of O vacancies.

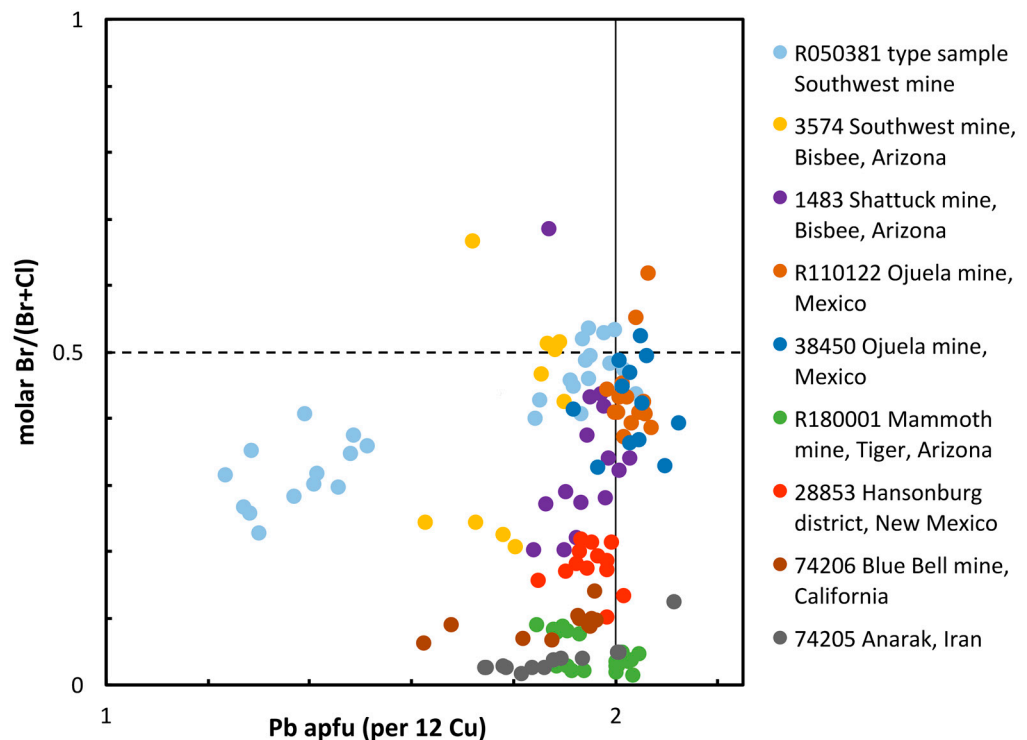


**Figure 4.** Plot of chemical data for murdochite–eddavidite from Table S1. Wide ranges of Pb/Cu and Br/(Br + Cl) are apparent. Points with molar Br/(Br + Cl) > 0.5 are eddavidite (above the dashed line), while those < 0.5 are murdochite.

This work found both eddavidite and murdochite in the Bisbee mining area, with molar Br/(Br + Cl) ranging from 0.21 to 0.69 (Tables 1 and S1). Two separate crystals from the type sample (Tables 1 and S1) give the following molar Br/(Br + Cl) values: lows of 0.23 and 0.24, highs of 0.53 and 0.64, and means of 0.39 and 0.53, respectively. Graeme sample 1483 from the Shattuck mine has the highest molar Br/(Br + Cl) seen in this study:

0.69 (Table S1). Nevertheless, Graeme sample 1483 is predominantly murdochite with mean molar  $\text{Br}/(\text{Br} + \text{Cl}) = 0.34$  (Table S1). Each spot analysis of Bisbee murdochite (and eddavidite) performed in this study revealed elevated Br (i.e.,  $\text{Br}/(\text{Br} + \text{Cl}) > 0.20$ ).

Eddavidite was also recognized in two murdochite samples from the Ojuela mine, Mexico: RRUFF sample R110122 has molar  $\text{Br}/(\text{Br} + \text{Cl})$  ranging from 0.37 to 0.62, with a mean of 0.44 (Table S1, Figure 3). NHMLAC 38450 has molar  $\text{Br}/(\text{Br} + \text{Cl})$  ranging from 0.33 to 0.52, with a mean of 0.42 (Table S1).

### 3.4. Zoning in Eddavidite–Murdochite

Zoning in murdochite has been noticed and discussed since 1970 [4,5]. This study finds no correlation between zoning under BSE and either Br content or molar  $\text{Br}/(\text{Br} + \text{Cl})$  ratio. Spots 61 and 71 on RRUFF sample R110122, murdochite–eddavidite from the Ojuela mine, have Br contents of 3.50 wt.% and 5.03 wt.%, respectively. Sample R110122 also has a significant range of molar  $\text{Br}/(\text{Br} + \text{Cl})$ : 0.62–0.37; nevertheless, it appears free of zoning (Figure 5). Notably, sample R110122 has <1% standard deviation in its  $\text{PbO}_2$  contents and appears rather homogenous in BSE imaging.

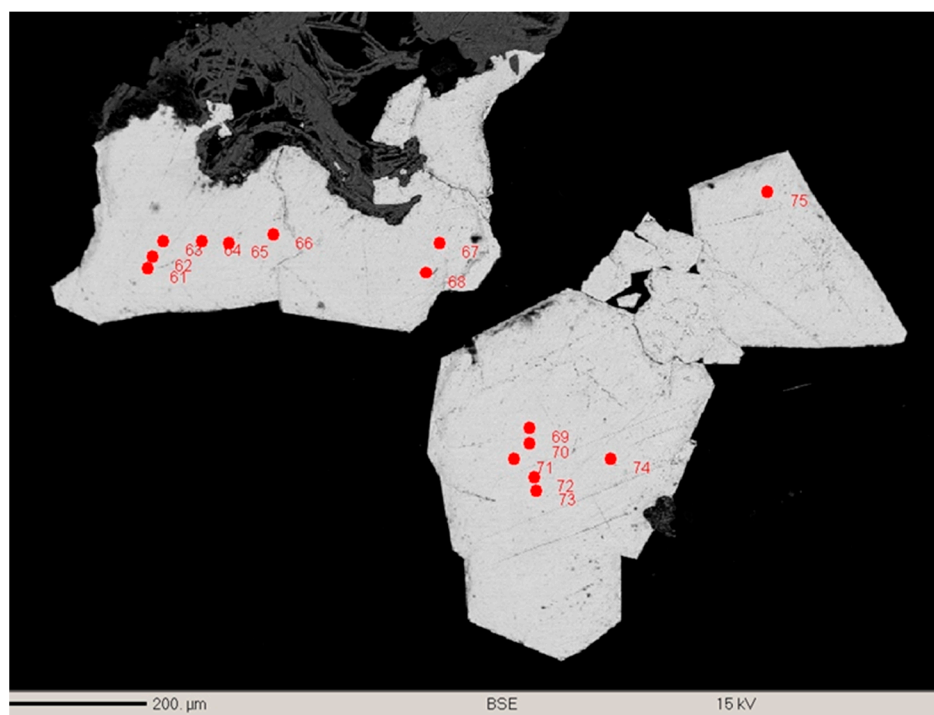


**Figure 5.** BSE image of mixed murdochite–eddavidite crystals from microprobe mount of RRUFF sample R110122. The dark material is associated aurichalcite. Note the homogeneity; this sample has rather consistent Pb values with standard deviation < 1% (Table S1). Locality: Ojuela mine, Mapimí, Durango, Mexico.

Zoning in eddavidite–murdochite seems to correlate with variations in  $\text{Pb}/\text{Cu}$  ratio. RRUFF sample R180001, murdochite from the Mammoth mine, shows pronounced zoning despite its low molar  $\text{Br}/(\text{Br} + \text{Cl})$  of 0.05 (Table S1, Figure 6). Spots 8 (lighter), 22 (darker), and 24 (darker) have Br contents of 0.26 wt.%, 0.29 wt.%, and 0.23 wt.%, respectively. Notably the spot with the intermediate Br content is lighter, while the spots with both higher and lower Br contents are darker. Tellingly, lighter zones have 32.0–32.4 wt.%  $\text{PbO}_2$ , while darker zones have 29.7–31.1 wt.%  $\text{PbO}_2$ . Sample R180001 exhibits 3% standard deviation in its  $\text{PbO}_2$  contents and displays conspicuous zoning in BSE imaging.

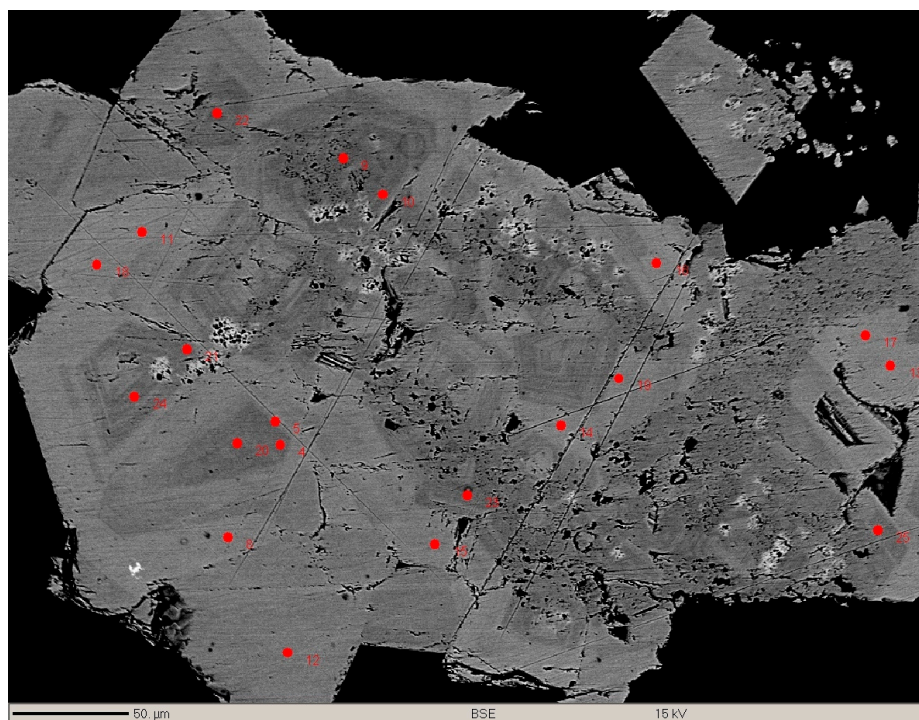


**Figure 6.** BSE imaging displays prominent zoning in murdochite from microprobe mount of RRUFF sample R180001. Lighter zones indicate elevated Pb contents; Pb contents have a standard deviation of 3% (Table S1). Locality: Mammoth mine (408 stope), Tiger, Pinal County, Arizona.

As previously proposed for murdochite in 1970 [4], zoning in mixed murdochite–eddauidite correlates with variable Pb/Cu. As the analyses reported herein are normalized to 12 Cu apfu, variable Pb/Cu simplifies to Pb apfu (Tables 1 and S1). In the case of R180001 (Table S1, Figure 6), the backscattered electron (BSE) contribution from  $\pm 0.06$  apfu Pb vs.  $\square$  ( $\Delta Z = 82$ ) certainly cancels out the BSE contribution from  $\pm 0.05$  apfu Br vs. Cl ( $\Delta Z = 18$ ). Considering both the strong BSE response of Pb and the established non-stoichiometry in the crystal structure [6], eddauidite cannot be distinguished from murdochite simply by BSE imaging.

### 3.5. Eddauidite Crystal Structure

The eddauidite crystal structure consists of interlinked square planar  $\text{CuO}_4$  units sharing edges with  $\text{PbO}_8$  cubes (Figure 7). Square planar  $\text{CuO}_4$  units are fundamental building blocks of tertiary  $\text{Cu}_{12}\text{O}_{24}$  metal clusters (Figure 8). A halogen atom (Br) sits at the center of the  $\text{Cu}_{12}\text{O}_{24}$  cluster. The Pb–O, Cu–O, and Cu–(Br,Cl) separations are 2.286(3) Å, 1.9245(7) Å, and 3.2671(3) Å, respectively.

The  $\text{Cu}_{12}\text{O}_{24}$  metal cluster in eddauidite (and isostructural murdochite) is a 26-sided polyhedron with 8 triangular faces and 18 square faces, which is known as a rhombicuboctahedron [26]. A decorated version of this metal cluster with composition  $\text{Cu}_{18}\text{O}_{24}$  is found in the structure of  $\text{BaCuO}_2$  [27].  $\text{Cu}_{12}\text{O}_{24}$  clusters in eddauidite (and murdochite) share faces to build a framework of ideal bulk composition  $\text{Cu}_3\text{O}_4$  (Figure 9).

Some chemical analyses show trace F (Table 1 and Table S1). As the anionic radius of  $\text{F}^-$  is much smaller than that of  $\text{Cl}^-$  or  $\text{Br}^-$  [28], trace F presumably substitutes for O. This is similar to the ordering of F and Cl–Br into distinct crystallographic sites as determined for claringbullite–barlowite [29,30], both of which occur at the type locality for eddauidite.

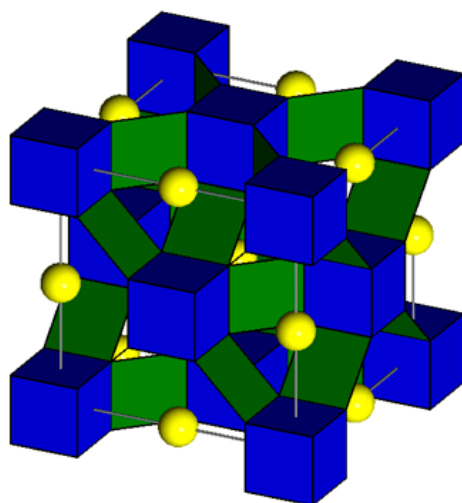


**Figure 7.** The eddavidite crystal structure tilted  $5^\circ$  off (211). Green squares, dark blue cubes, and yellow spheres represent  $\text{CuO}_4$ ,  $\text{PbO}_8$ , and Br, respectively.

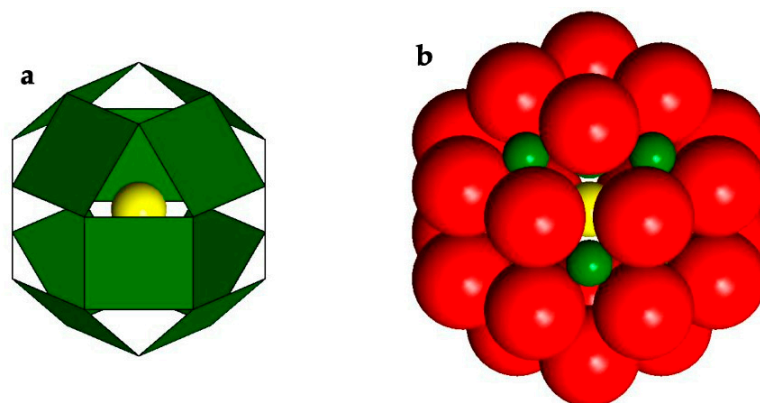


**Figure 8.** The  $\text{Cu}_{12}\text{O}_{24}$  metal-oxide cluster in eddavidite and murdochite. (a) Polyhedral view comprising 12 square planar  $\text{CuO}_4$  units sharing vertices to build a rhombicuboctahedron; a single yellow halogen is enclosed. (b) Space filling view with red O, green Cu, and yellow halogen. Both renderings have the same scale, viewed along [332].

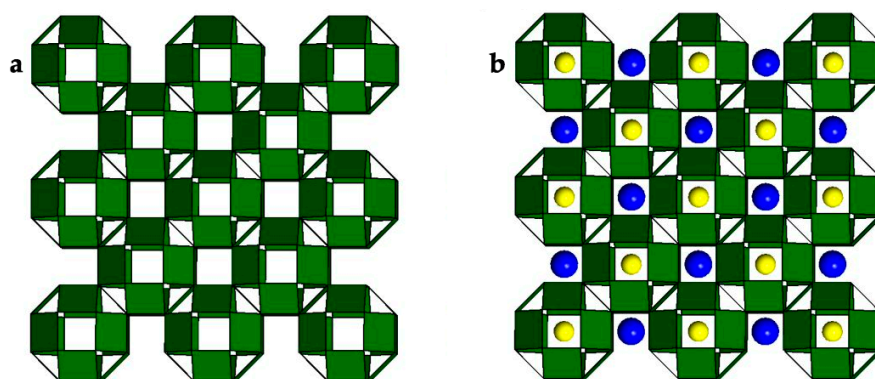


**Figure 9.** Slab of the eddavidite–murdochite crystal structure tilted  $5^\circ$  off [001]. (a) A “house of cards” of square planar  $\text{CuO}_4$  units share vertices to build a framework of ideal composition  $\text{Cu}_3\text{O}_4$ . (b) Blue Pb and yellow halogen atoms decorate the  $\text{Cu}_3\text{O}_4$  framework. The identity of the halogen, Br in eddavidite vs. Cl in murdochite, is the singular distinction between the two species.

## 4. Discussion

### 4.1. Origin of Eddavidite

This study reports eddavidite from two separate mining areas: Bisbee, Arizona, USA, and Mapimí, Durango, Mexico. Both mining areas exploit large carbonate replacement systems, with Bisbee relatively richer in Cu than Pb-Zn-Ag [18,19], whereas Mapimí is richer in Pb-Zn-Ag than Cu [21–23]. Despite their overland separation of ~850 km, Bisbee and Mapimí share a significant chapter of geological history. Between 105 and 85 Ma, both localities were submerged in the paleo-oceanic Western Interior Seaway [31,32]. The subsequent orogeny of the Sierra Madre Occidental left Bisbee and Mapimí in separate watersheds, specifically the endorheic Bolson de Mapimí and the Bisbee Basin [33]. Presumably these basins trapped seawater from the Western Interior Seaway, which eventually desiccated.

When halite precipitates from seawater, its crystalline lattice does not readily accommodate Br, leaving behind residual brines relatively enriched in Br [34–36]. Evaporation of seawater increases molar Br/Cl by a factor of ~6.5 in residual brines [36]. In open basins, Cl washes into ground waters, progressively removing Cl but leaving Br, all the while increasing residual Br/Cl [36,37]. Bromine enriched sediments develop by this cyclical process.

At Earth's surface, bromine is significantly rarer than chlorine. The upper continental crust has molar Br/Cl ~0.0019 [38], and seawater has molar Br/Cl ~0.0015 [36]. Hydrothermal solutions have Br/Cl ~1:10,000 [39]. The relative insolubilities of bromides compared to those of chlorides promote bromide mineral formation. For instance,  $K_{sp}$  values for  $PbBr_2$  and  $PbCl_2$  are  $6.6 \times 10^{-6}$  and  $1.59 \times 10^{-5}$ , respectively. Greater insolubility for eddavidite than for murdochite would favor eddavidite deposition from fluids with  $[Cl] > [Br]$ . Eddavidite formation arises from both the hydrological process concentrating Br in trapped paleo-seawater and its presumed relative insolubility compared to murdochite.

### 4.2. Bromine-Bearing Minerals

The IMA mineral list currently has 15 species with Br in their formulae, 11 of which contain essential Br (Table 6). Three species with essential Br occur at Bisbee: eddavidite, bromargyrite, and barlowite; all of these have more common Cl analogs: murdochite, chlorargyrite, and claringbullite. All six of these species occur at Bisbee and together they constitute three pairs of chloride-bromide mineral analogs.

**Table 6.** Current listing of IMA approved mineral species with Br in their formulae, those with essential Br are listed in bold.

Mineral	IMA Chemistry	Cl Analog	Reference
<b>barlowite</b>	$Cu_4BrF(OH)_6$	claringbullite	[29]
<b>bromargyrite</b>	AgBr	chlorargyrite	[40]
<b>comancheite</b>	$Hg^{2+}_{55}N^{3-}_{24}(NH_2,OH)_4(Cl,Br)_{34}$	–	[41]
<b>demicheleite-(Br)</b>	BiSBr	demicheleite-(Cl)	[42]
<b>eddavidite</b>	$Pb_2Cu_{12}O_{15}Br_2$	murdochite	this study
<b>ermakovite</b>	$(NH_4)(As_2O_3)_2Br$	–	[43]
<b>grechishchevite</b> †	$Hg_3S_2BrCl_{0.5}I_{0.5}$	–	[44]
<b>kadyrelite</b>	$([Hg^{1+}]_2)_3OBr_3(OH)$	eglestonite	[45]
<b>kelyanite</b>	$Hg_{12}SbO_6BrCl_2$	–	[46]
<b>kuzminite</b>	HgBr	calomel	[47]
lucabindiite *	$(K,NH_4)As_4O_6(Cl,Br)$	–	[48]
mutnovskite *	$Pb_2AsS_3(I,Cl,Br)$	–	[49]
perroudite *	$Ag_4Hg_5S_5(I,Br)_2Cl_2$	–	[50]
tedhadleyite *	$Hg^{2+}Hg^{1+}_{10}O_4I_2(Cl,Br)_2$	–	[51]
<b>vasilyevite</b>	$(Hg_2)^{2+}_{10}O_6I_3Br_2Cl(CO_3)$	–	[52]

\* Br subordinate to Cl in mixed halogen sites determined by crystal structure solution; † Crystal structure not refined, but empirically molar Br > (I + Cl).

Eddavidite is the first species with essential Br reported from Mapimí, where it occurs in contact with its Cl analog murdochite. The chloride species claringbullite [29] and chlorargyrite [22] are both recorded at Mapimí, and both species have known bromide analogs, but neither of the Br species has yet been recorded there. Chlorargyrite is visually nondescript at Mapimí, occurring within oxidized silver-lead ores, which are expeditiously sold off for smelting. Interestingly, Mapimí chlorargyrite contains elevated Br [22]. Further examination of Mapimí specimens may complete the chloride-bromide species pairs seen at Bisbee, thus increasing mineralogical correlations between the two mining areas. The Bisbee mining area constitutes the most mineralogically diverse province in Arizona, with 330 recorded species [53], while the Ojuela mine complex at Mapimí has 142 species (mindat.org), which is less than half of the count recorded at Bisbee.

#### 4.3. Identifying Eddavidite

Eddavidite cannot be distinguished from murdochite visually, nor by BSE imaging, nor by X-ray powder diffraction. At present, only chemical analyses can reliably confirm eddavidite.

**Supplementary Materials:** The following supporting information can be downloaded at: <https://www.mdpi.com/article/10.3390/min14030307/s1>, Table S1: Chemistry of mixed eddavidite–murdochite and murdochite; eddavidite.cif containing crystal structure solution and structure factors.

**Author Contributions:** Conceptualization, R.T.D. and M.J.O.; methodology, M.R.; validation, M.J.O. and M.R.; formal analysis, M.J.O. and M.R.; investigation, M.R.; resources, R.T.D., R.G.III, R.G.IV and D.G.; data curation, M.R., R.G.III, R.G.IV and D.G.; writing—original draft preparation, M.R. and R.G.III; writing—review and editing, M.R., M.J.O. and R.T.D.; visualization, M.R. and M.J.O.; supervision, R.T.D.; funding acquisition, M.R. and R.T.D. All authors have read and agreed to the published version of the manuscript.

**Funding:** Funding for this research was provided by two generous donations to the University of Arizona. Allan Norville provided funding for a research assistantship in mineralogy and mineral museum studies under the Department of Geosciences, which supported the senior author. Richard Graeme III provided funding for electron microprobe analysis.

**Data Availability Statement:** The original contributions presented in the study are included in the article/Supplementary Materials, further inquiries can be directed to the corresponding author or the RRUFF™ Project at <https://ruff.info/> (accessed on 2 March 2024).

**Acknowledgments:** We thank Aaron Celestian, Alyssa Morgan, George Harlow, and Jamie Newman for supplying samples. We thank Stan Esbenshade for donating what became the type specimen of eddavidite to the University of Arizona Mineral Museum. Ken Domanik instructed and assisted in electron microprobe analysis. The authors thank Richard Graeme III for providing funding for this research. We thank Zak Jibrin for assisting with electron microprobe sample preparation and Dominique “Nicky” Geisler for assisting with SEM operation. Jim McGlasson and James Lyons provided excellent discussion on the tectonic situation between Bisbee and Mapimí. Hexiong Yang made the initial discovery of eddavidite and proposed the species to the IMA. We dedicate this study to author Richard Graeme III (1941–2021), the geologist, the mining engineer, the historian, whose unmatched expertise in Bisbee mineralogy will be missed by the mineralogical community. The Graeme family’s well-documented Bisbee exploration records and collections will fuel scientific research for years to come.

**Conflicts of Interest:** Author Richard Graeme III provided partial funding for this research, while also contributing to the occurrence section in Bisbee, AZ. However, the Graeme family authors had no role in the design of the study; nor in the collection, analyses, or interpretation of data; nor in the decision to publish the results.

## References

1. Christ, C.L.; Clark, J.R. Crystal structure of murdochite (abstract). *Am. Mineral.* **1954**, *39*, 321.
2. Fahey, J.J. Murdochite, a new copper lead oxide mineral. *Am. Mineral.* **1955**, *40*, 905–906.
3. Christ, C.L.; Clark, J.R. The crystal structure of murdochite. *Am. Mineral.* **1955**, *40*, 907–916.

4. Adib, D.; Otteman, J. Some new lead oxide minerals and murdochite from T. Khuni mine, Anarak, Iran. *Miner. Depos.* **1970**, *5*, 86–93. [[CrossRef](#)]
5. Burke, E.A.J.; Maaskant, P. New data on murdochite. *Neues Jb. Miner. Monat.* **1970**, 558–565.
6. Dubler, E.; Verdani, A.; Oswald, H.R. New structure determination of murdochite,  $\text{Cu}_6\text{PbO}_8$ . *Acta Crystallogr.* **1983**, *C39*, 1143–1146. [[CrossRef](#)]
7. Taguchi, H. Relationship between crystal structure and electrical properties of murdochite-type  $\text{Ni}_{6+2x}\text{Mn}_{1-x}\text{O}_8$ . *Solid State Commun.* **1998**, *108*, 635–639. [[CrossRef](#)]
8. Hayakawa, H.; Akiba, E.; Ono, S.; Ihara, H.; Izumi, F.; Asano, H. Refinement of the crystal structures of  $\text{Cu}_6\text{O}_8\text{InCl}$  and  $\text{Cu}_6\text{O}_8\text{Cu}_2\text{Cl}$  by neutron powder diffraction. *J. Ceram. Soc. Jpn.* **1993**, *101*, 745–751. [[CrossRef](#)]
9. Zouganelis, G.; Bushida, K.; Yazawa, I.; Terada, N.; Jo, M.; Hayakawa, H.; Ihara, H. Structure refinement of the  $\text{Cu}_6\text{O}_8 \cdot \text{YCl}$  compound. *Solid State Commun.* **1991**, *80*, 709–713. [[CrossRef](#)]
10. Müller, M.; Thiele, G.; Zöllner, C. Strukturparameter von  $\text{TlPd}_3\text{O}_4$  aus einem Neutronen-Pulverdiagramm. *Z. Anorg. Allg. Chem.* **1978**, *443*, 19–22. [[CrossRef](#)]
11. Winkler, B.; Chall, M.; Pickard, C.J.; Milman, V.; White, J. Structure of  $\text{Cu}_6\text{PbO}_8$ . *Acta Crystallogr.* **2000**, *B56*, 22–26. [[CrossRef](#)]
12. Roberts, S.; David, E.E., Jr. Who elevated science under Nixon, dies at 92. *New York Times*, 28 February 2017; Section B. p. 13.
13. Wilson, W.E.; Bartsch, J.A.; Mauthner, M. *Masterpieces of the Mineral World*; The Houston Museum of Natural Science and the Mineralogical Record, Inc.: Tucson, AZ, USA, 2004; 264p.
14. Pouchou, J.L.; Pichoir, F. Un nouveau modèle de calcul pour la micro-analyse quantitative par spectrométrie de rayons X. Partie I: Application à l'analyse d'échantillons homogènes. *Rech. Aéropatiale* **1984**, *3*, 167–192.
15. Hawthorne, F.C.; Oberti, R.; Harlow, G.E.; Maresch, W.V.; Martin, R.F.; Schumacher, J.C.; Welch, M.D. Nomenclature of the amphibole supergroup. *Am. Mineral.* **2012**, *97*, 2031–2048. [[CrossRef](#)]
16. Downs, R.T.; Bartelmehs, K.L.; Gibbs, G.V.; Boisen, M.B.J. Interactive software for calculating and displaying X-ray or neutron powder diffractometer patterns of crystalline materials. *Am. Mineral.* **1993**, *78*, 1104–1107.
17. Sheldrick, G.M. A short history of SHELX. *Acta Crystallogr.* **2008**, *A64*, 112–122. [[CrossRef](#)]
18. Graeme, R.W. Famous mineral localities, Bisbee, Arizona. *Mineral. Rec.* **1981**, *12*, 258–319.
19. Graeme, R. Bisbee revisited. *Mineral. Rec.* **1993**, *24*, 421–436.
20. Lang, J.R.; Thompson, J.F.H.; Mortensen, J.K.; Baker, T.; Coulson, I.; Duncan, R.A.; Maloof, T.L.; James, J.; Friedman, R.M.; Lepitre, M.E. *Regional and System-Scale Controls on the Formation of Copper and/or Gold Magmatic-Hydrothermal Mineralization*; Mineral Deposit Research Unit Special, University of British Columbia: Vancouver, BC, Canada, 2001; Volume 2, 115p.
21. Panczner, W.D. *Minerals of Mexico*; Van Nostrand Reinhold: New York, NY, USA, 1987; 459p.
22. Hoffmann, V.J. The Mineralogy of the Mapimí Mining District, Durango, Mexico. Ph.D. Thesis, University of Arizona, Tucson, AZ, USA, 1967; 230p.
23. Moore, T.P.; Megaw, P.K.M. Mexico II. The Ojuela mine. *Mineral. Rec.* **2003**, *34*, 1–120.
24. Switzer, G. Paradamite, a new zinc arsenate from Mexico. *Science* **1956**, *123*, 1039. [[CrossRef](#)]
25. Taggart, J.E.; Foord, E.E.; Rosenzweig, A.; Hanson, T. Scrutinyite, natural occurrences of  $\alpha\text{PbO}_2$  from Bingham, New Mexico, U.S.A., and Mapimi, Mexico. *Can. Mineral.* **1988**, *26*, 905–910.
26. Núñez-Regueiro, M.D.; Núñez-Regueiro, M. Folding  $\text{CuO}_2$  planes into fullerene-like clusters. *J. Phys. I* **1994**, *4*, 169–174.
27. Paulus, E.F.; Miehle, G.; Fuess, H.; Yehia, I.; Löchner, U. The crystal structure of  $\text{BaCuO}_2$ . *J. Solid State Chem.* **1991**, *90*, 17–26. [[CrossRef](#)]
28. Shannon, R.D. Revised effective ionic radii and systematic study of interatomic distances in halides and chalcogenides. *Acta Crystallogr.* **1976**, *A32*, 751–767. [[CrossRef](#)]
29. Welch, M.D.; Najorka, J.; Rumsey, M.S.; Spratt, J. The hexagonal  $\leftrightarrow$  orthorhombic structural phase transition in claringbullite,  $\text{Cu}_4\text{FCl}(\text{OH})_6$ . *Can. Mineral.* **2021**, *59*, 265–285. [[CrossRef](#)]
30. Elliott, P.; Cooper, M.A.; Pring, A. Barlowite,  $\text{Cu}_4\text{FBr}(\text{OH})_6$ , a new mineral isostructural with claringbullite: Description and crystal structure. *Mineral. Mag.* **2014**, *78*, 1755–1762. [[CrossRef](#)]
31. Slattery, J.S.; Cobban, W.A.; McKinney, K.C.; Harries, P.J.; Sandness, A.L. Early Cretaceous to Paleocene paleogeography of the Western Interior Seaway of North America and its relation to tectonics and eustasy. In *Cretaceous Conference: Evolution and Revolution*; Bingle-Davis, M., Ed.; Wyoming Geological Association: Casper, WY, USA, 2015; pp. 22–60.
32. Blakely, R.C.; Ranney, W.D. *Ancient Landscapes of Western North America*; Springer: Berlin/Heidelberg, Germany, 2018; 228p.
33. Dickinson, W.R.; Klute, M.A.; Swift, P.N. The Bisbee basin and its bearing on late Mesozoic paleogeographic and paleotectonic relations between the cordilleran and caribbean regions. In *Cretaceous Stratigraphy Western North America*; Abbott, P.L., Ed.; Pacific Section, Society of Economic Paleontologists and Mineralogists: Los Angeles, CA, USA, 1986; pp. 51–62.
34. Braitsch, O. *Salt Deposits: Their Origin and Composition*; Springer: New York, NY, USA, 1971; 297p.
35. McCaffrey, M.A.; Lazar, B.; Holland, H.D. The evaporation path of seawater and coprecipitation of  $\text{Br}^-$  and  $\text{K}^+$  with halite. *J. Sediment. Petrol.* **1987**, *57*, 928–937.
36. Babel, M.; Schreiber, B.C. Geochemistry of evaporites and evolution of seawater. In *Treatise on Geochemistry*, 2nd ed.; Holland, H.D., Turekian, K.K., Eds.; Elsevier: Amsterdam, The Netherlands, 2014; Volume 9, pp. 483–560.
37. Sanford, W.E.; Wood, W.W. Brine evolution and mineral deposition in hydrologically open evaporite basins. *Am. J. Sci.* **1991**, *291*, 687–710. [[CrossRef](#)]

38. Rudnick, R.L.; Gao, S. Composition of the continental crust. In *Treatise on Geochemistry*, 2nd ed.; Holland, H.D., Turekian, K.K., Eds.; Elsevier: Amsterdam, The Netherlands, 2014; Volume 4, pp. 1–51.
39. Barnes, H.L. (Ed.) *Geochemistry of Hydrothermal Ore Deposits*, 3rd ed.; Wiley and Sons: New York, NY, USA, 1997; 992p.
40. Palache, C.; Berman, H.; Frondel, C. *Dana's System of Mineralogy*, 7th ed.; John Wiley & Sons: New York, NY, USA, 1951; Volume II, 1124p.
41. Cooper, M.A.; Abdu, Y.A.; Hawthorne, F.C.; Kampf, A.R. The crystal structure of comancheite,  $\text{Hg}^{2+}_{55}\text{N}^{3-}_{24}(\text{OH},\text{NH}_2)_4(\text{Cl},\text{Br})_{34}$  and crystal-chemical and spectroscopic discrimination of  $\text{N}^{3-}$  and  $\text{O}^{2-}$  anions in  $\text{Hg}^{2+}$  compounds. *Mineral. Mag.* **2013**, *77*, 3217–3237. [[CrossRef](#)]
42. Demartin, F.; Gramaccioli, C.M.; Campostrini, I.; Orlandi, P. Demicheleite,  $\text{BiSBr}$ , a new mineral from La Fossa crater, Vulcano, Aeolian Islands, Italy. *Am. Mineral.* **2008**, *93*, 1603–1607. [[CrossRef](#)]
43. Karpenko, V.Y.; Pautov, L.A.; Siidra, O.I.; Mirakov, M.A.; Zaitsev, A.N.; Plechov, P.Y.; Makhmadsharif, S. Ermakovite  $(\text{NH}_4)(\text{As}_2\text{O}_3)_2\text{Br}$ , a new exhalative arsenite bromide mineral from the Fan-Yagnob coal deposit, Tajikistan. *Mineral. Mag.* **2023**, *87*, 69–78. [[CrossRef](#)]
44. Vasil'ev, V.I.; Usova, L.V.; Pal'chik, N.A. Grechishchevite— $\text{Hg}_3\text{S}_2(\text{Br},\text{Cl},\text{I})_2$ —A new supergene mercury sulfohalide. *Geol. Geofiz.* **1989**, *30*, 61–69. (In Russian)
45. Vasil'ev, V.I. Kadyrelite,  $\text{Hg}_4(\text{Br},\text{Cl})_2\text{O}$ —A new oxyhalide of mercury from the Kadyrelsky ore deposit (Tuvinskaya ASSR). *Zap. Vsesoyuznogo Mineral. Obs.* **1987**, *116*, 733–737. (In Russian)
46. Pervukhina, N.V.; Borisov, S.V.; Magarill, S.A.; Naumov, D.Y.; Vasil'ev, V.I. The crystal structure of kelyanite,  $(\text{Hg}_2)_6(\text{SbO}_6)\text{BrCl}_2$ . *Am. Mineral.* **2008**, *93*, 1666–1669. [[CrossRef](#)]
47. Vasil'ev, V.I.; Lavrent'ev, Y.G.; Pal'chik, N.A. Kuzminite— $\text{Hg}_2(\text{Br},\text{Cl})_2$ —A new natural halide of mercury. *Zap. Vsesoyuznogo Mineral. Obs.* **1986**, *115*, 595–598. (In Russian)
48. Garavelli, A.; Mitolo, D.; Pinto, D.; Vurro, F. Lucabindiite,  $(\text{K},\text{NH}_4)\text{As}_4\text{O}_6(\text{Cl},\text{Br})$ , a new fumarole mineral from the “La Fossa” crater at Vulcano, Aeolian Islands, Italy. *Am. Mineral.* **2013**, *98*, 470–477. [[CrossRef](#)]
49. Zelenski, M.; Balić-Žunić, T.; Bindi, L.; Garavelli, A.; Makovicky, E.; Pinto, D.; Vurro, F. First occurrence of iodine in natural sulfosalts: The case of mutnovskite,  $\text{Pb}_2\text{AsS}_3(\text{I},\text{Cl},\text{Br})$ , a new mineral from the Mutnovsky volcano, Kamchatka Peninsula, Russian Federation. *Am. Mineral.* **2006**, *91*, 21–28. [[CrossRef](#)]
50. Mumme, W.G.; Nickel, E.H. Crystal structure and crystal chemistry of perroudite: A mineral from Coppin Pool, Western Australia. *Am. Mineral.* **1987**, *72*, 1257–1262.
51. Cooper, M.A.; Hawthorne, F.C. The crystal structure of tedhadleyite,  $\text{Hg}^{2+}\text{Hg}^{1+}_{10}\text{O}_4\text{I}_2(\text{Cl},\text{Br})_2$ , from the Clear Creek Claim, San Benito County, California. *Mineral. Mag.* **2009**, *73*, 227–234. [[CrossRef](#)]
52. Cooper, M.A.; Hawthorne, F.C. The crystal structure of vasilyevite,  $(\text{Hg}_2)^{2+}_{10}\text{O}_6\text{I}_3(\text{Br},\text{Cl})_3(\text{CO}_3)$ . *Can. Mineral.* **2003**, *41*, 1173–1181. [[CrossRef](#)]
53. Graeme, R.W., III; Graeme, R.W., IV; Graeme, D.L. *The Mineralogy of Bisbee, Arizona*; Copper Czar Publishing: Bisbee, AZ, USA, 2021; Volume I.

**Disclaimer/Publisher's Note:** The statements, opinions and data contained in all publications are solely those of the individual author(s) and contributor(s) and not of MDPI and/or the editor(s). MDPI and/or the editor(s) disclaim responsibility for any injury to people or property resulting from any ideas, methods, instructions or products referred to in the content.